More efficient repair of DNA double-strand breaks in skeletal muscle stem cells compared to their committed progeny

Leyla Vahidi Ferdousi, Pierre Rocheteau, Romain Chayot, Benjamin Montagne, Zayna Chaker, Patricia Flamant, Shahragim Tajbakhsh, Miria Ricchetti

PII: S1873-5061(14)00094-4
DOI: doi: 10.1016/j.scr.2014.08.005
Reference: SCR 464

To appear in: *Stem Cell Research*

Received date: 4 October 2013
Revised date: 14 July 2014
Accepted date: 15 August 2014

Please cite this article as: Ferdousi, Leyla Vahidi, Rocheteau, Pierre, Chayot, Romain, Montagne, Benjamin, Chaker, Zayna, Flamant, Patricia, Tajbakhsh, Shahragim, Ricchetti, Miria, More efficient repair of DNA double-strand breaks in skeletal muscle stem cells compared to their committed progeny, *Stem Cell Research* (2014), doi: 10.1016/j.scr.2014.08.005

More efficient repair of DNA double-strand breaks in skeletal muscle stem cells compared to their committed progeny

Leyla Vahidi Ferdousi[1], Pierre Rocheteau[2*], Romain Chayot[1*], Benjamin Montagne[1], Zayna Chaker[1], Patricia Flamant[2], Shahragim Tajbakhsh[2] and Miria Ricchetti[1‡]

*Equal contributing authors

‡Corresponding author: (mricch@pasteur.fr), +33 1 4568 8567

[1]Institut Pasteur, Yeast Molecular Genetics, Dept. of Genomes and Genetics and CNRS UMR3525, [2]Institut Pasteur, Stem Cells & Development, Dept. of Developmental Biology and Stem Cells and CNRS URA 2578, 25 rue du Dr. Roux, 75724 Paris Cedex 15, France.

Present addresses: Romain Chayot, Global Bioenergies, Evry, France; Pierre Rocheteau and Patricia Flamant, Institut Pasteur, Human Histopathology and Animal Models; Zayna Chaker, Centre de Recherche Saint-Antoine, INSERM-UPMC S938, Paris France

Running title: Efficient repair of DSBs in muscle stem cells

Keywords: DNA damage, differentiation, muscle, stem cells, quiescence, NHEJ

Abstract

The loss of genome integrity in adult stem cells results in accelerated tissue aging and possibly cancerogenesis. Adult stem cells in different tissues appear to react robustly to DNA damage. We report that adult skeletal stem (satellite) cells do not primarily respond to radiation-induced DNA double-strand breaks (DSBs) via differentiation and exhibit less apoptosis compared to other myogenic cells. Satellite cells repair these DNA lesions more efficiently than their committed progeny. Importantly, non-proliferating satellite cells and post-mitotic nuclei in the fibre exhibit dramatically distinct repair efficiencies. Altogether, reduction of the repair capacity appears to be more a function of differentiation than of the proliferation status of the muscle cell. Notably, satellite cells retain high efficiency of DSB repair also when isolated from the natural niche. Finally, we show that repair of DSB substrates is not only very efficient but, surprisingly, also very accurate in satellite cells and that accurate repair depends on the key non-homologous end-joining factor DNA-PKcs.

Introduction

Stem cells play crucial roles in tissue growth, homeostasis and regeneration. The self-renewal capacity of stem cells and their potential to maintain the tissue, depends on their ability to regulate endogenous and exogenous (*e.g.* irradiation) genotoxic stress. The accumulation of DNA damage and consequent loss of genome integrity due to double strand breaks (DSBs) is one of the major causes of apoptosis, senescence and aging, including in stem cells (Lombard et al., 2005; Nijnik et al., 2007; Rossi et al., 2007; Ruzankina et al., 2008). In the small intestine, stem cells at the bottom of the crypt are proliferating and radioresistant, whereas those around the +4 position are quiescent and radiosensitive (Hua et al., 2012; Li and Clevers, 2010; Potten et al., 2009), therefore the response of stem cells to DNA damage can be distinct depending on their origin, cell cycle status, or both. In another report, melanocyte stem cells did not undergo detectable ionizing radiation (IR)-induced apoptosis, but the stem cell niche was depleted due to their differentiation (Inomata et al., 2009).

Inefficient DNA DSB repair can promote genomic rearrangements which can lead to malignant transformations (Reya et al., 2001) thus leading to the notion that stem cells with compromised genome integrity commit altruistic suicide or differentiate, and are more sensitive to DNA damage than other cells. However, hair-follicle-bulge stem cells are resistant to DNA damage-induced apoptosis, largely mediated by higher expression of anti-apoptotic *Bcl-2* (Sotiropoulou et al., 2010). Moreover, highly enriched hematopoietic stem and progenitor cells (HSPCs) express more anti-apoptotic genes (but not *Bcl-2*) and less pro-apoptotic genes (but not *Bim*) than myeloid progenitors (Mohrin et al., 2010). In a context of reduced apoptosis, proficient and accurate DSB repair is necessary to assure that survivor cells do not incur genome instability and deleterious mutations (Chapman et al., 2012). Interestingly, hair-follicle-bulge stem cells display a faster DNA repair than other basal epidermal cells (Sotiropoulou, et al., 2010). HSPCs cells also display efficient DSB repair but

this is frequently associated with genome rearrangements (Mohrin, et al., 2010). Adult stem cells and their derived tissues display different sensitivity to radiation-induced DNA damage (Blanpain et al., 2011), suggesting that they might respond differently to genotoxic injury. Unresolved questions include whether other stem cells are simultaneously more apoptosis-resistant and DNA repair prone than differentiated cells, and whether high occurrence of mutations is the necessary output for efficient DSB repair in stem cells.

Differences in repair efficiency and accuracy could be ascribed to distinct repair mechanisms associated with cell cycle phase. Proliferating cells rely essentially on accurate recombination-dependent repair (HR, homologous recombination), acting mostly during S/G2 (Chapman, et al., 2012). In contrast, non-dividing cells rely essentially on non-homologous end-joining (NHEJ), which is active during the entire cell cycle. NHEJ joins the broken ends and displays some inaccuracy depending on the type of DNA ends (Wyman and Kanaar, 2006). In agreement with this notion, quiescent HSPCs express lower levels of HR-associated repair factors and higher levels of NHEJ markers than proliferating HSPCs (Mohrin, et al., 2010).

Skeletal muscle growth and regeneration is effected by satellite (stem) cells that have robust regenerative potential and are quiescent in the adult. After muscle injury, they enter the cell cycle and produce myoblasts that fuse to effect muscle regeneration. Satellite cells subsequently self-renew in their niche, which is located between the myofibre plasmalemma and the basement membrane. Transcription factors including the homeobox/paired domain gene *Pax7*, the myogenic determination genes *Myf5* and *Myod*, and the differentiation gene *Myogenin* play critical roles in satellite cell regulation (Relaix and Zammit, 2012; Tajbakhsh, 2009). The well-defined stages of lineage progression as well as markers and morphological readouts for distinguishing the distinct cell states from stem to differentiated cells provide an

ideal system to investigate how stem cells and their progeny in this tissue respond to IR-induced genotoxic stress. Previous studies showed that high-doses of irradiation (18-25 Gy) compromise satellite cell function and muscle regeneration (Boldrin et al., 2012; Gayraud-Morel et al., 2009; Gross and Morgan, 1999; Heslop et al., 2000; Pagel and Partridge, 1999; Wakeford et al., 1991). Muscle regeneration in response to genotoxic stress is affected by a variety of factors, as muscle damage rescues proliferation of some myogenic cells after high doses of limb irradiation (Gross and Morgan, 1999; Heslop, et al., 2000). Moreover, preservation of the niche has a key role in muscle regeneration during engraftment (Boldrin, et al., 2012), which is also significantly affected by non-myogenic cells like macrophages (Saclier, Yacoub-Youssef, et al., 2013). Regeneration in normal and irradiated muscle relies on multiple cell types and cell-cell signaling, however the relative contribution of these cells remains unknown. Therefore a systematic analysis of each cell type is critical to understand how regeneration occurs after irradiation. Here, we show that skeletal muscle stem cells exhibit a robust DNA repair machinery, and that they effect IR-induced DSB repair significantly better than their committed progeny, and with higher accuracy. Further, the proliferation status of cells appears to affect the repair efficiency to a lower extent than does differentiation. Finally, we show that the niche does not significantly affect the repair efficiency of muscle stem cells pointing to a cell autonomous role for DNA repair.

Materials and methods

Ethics statement

All animal work was performed according to national and European guidelines.

Immunofluorescence and imaging

Cells and myofibres were fixed as described previously (Gayraud-Morel et al., 2007). Cryosections of the TA muscle were obtained and treated as described (Gayraud-Morel et al., 2012). Antibodies and immunocytochemistry reagents are described (Jory et al., 2009). Rabbit polyclonal antibody anti-53BP1 (Novus Biologicals); anti-phosphohistone H2A.X (Ser139) mouse monoclonal (Upstate). Images were acquired with a Zeiss Axioplan equipped with an Apotome and Axiovision software, or a LEICA SPE confocal and LAS software. In isolated cells and fibres, counting of foci was performed on the total cell volume, whereas in muscle cross-sections foci were counted in the plane of section. All images were assembled in Adobe Photoshop or Image J. Some images were assembled as projections of successive confocal acquisitions.

FACS and cell culture

Muscles were dissected and digested in 0.1% Collagenase and 0.25% Trypsin to form a slurry, as described (Gayraud-Morel, et al., 2007), that was then sorted by FACS based on GFP epifluorescence of *Tg:Pax7-nGFP* mice using FACSAria, BD or MoFlo, and the FACSDiva software. Myoblasts were isolated after injuries performed by intramuscular injections of 10 µl of 10 µg/ml snake venom notexin (Notexin, Lotaxan) on anesthetized mice (0.5% Imalgene/2% Rompun) and TA muscles were collected 5 days post-injury then purified by FACS. For cell culture, cells were plated on Matrigel coated dishes in 1:1 DMEM (Invitrogen) to MCDB201 (Sigma) containing 20% fœtal calf serum (FCS) (Invitrogen) and Ultroser (Gayraud-Morel, et al., 2007). To allow differentiation, the culture was maintained

for 10-11 days without changing the medium. Primary wild type MEFs were cultured in DMEM medium (Dulbecco's modified Eagle's medium, Gibco) supplemented with 10% foetal calf serum (Gibco), 1mM sodium pyruvate and 50 µg/ml gentamicin at 37°C with 5% CO_2 and 20% O_2. When indicated, NU7441 (Axon Medchem) dissolved in DMSO, was added at a final concentration of 10µM, and control experiments were performed in the presence of DMSO alone. Cells were pre-treated with NU7441 for 4h, as described (Smith et al., 2001), and subsequently maintained in medium containing the drug dissolved in DMSO or an equivalent volume of DMSO for the duration of the experiment.

Single-fibre preparation

Single fibres were prepared as described previously (Gayraud-Morel, et al., 2012). The procedure is described in detail in the Supplementary material.

Irradiation

Total body, myofibre, and cell irradiation were performed with a ^{137}Cs Irradiateur IBL637 (CIS Biointernational). A single irradiation of 5 Gy was delivered, unless otherwise indicated (20 Gy). When indicated, three rounds of 2 Gy each or 5 Gy each were delivered at either day.

RNA extraction, RT and qPCR.

Standard RNA extraction and RT-qPCR techniques have been used. They are detailed in the Supplementary material.

Single-cell electrophoresis or comet assay

Pax7-GFP^+ satellite cells (untreated muscle) and myoblasts (notexin-injured muscle) from irradiated (5 Gy) and non-irradiated mice were isolated by FACS 2h post-IR and immediately used for neutral comet assay. For this, cells were embedded in agarose on slides, as previously

described (Olive and Banath, 2006). The olive moment is calculated as Tail DNA (%) x Tail Moment length.

Statistical relevance of observed differences

The number of foci in myoblasts, and satellite and differentiated cells on fibres was counted in ≥150 cells totally, originated from 3-5 mice. Statistical analysis of two cell populations was performed with the unpaired t test. For qPCR analysis of the expression of a gene in satellites, myoblasts and myotubes, data were first analysed with the Two-Way ANOVA (with Bonferroni test) using the software Prism; differentiation and irradiation were used as independent variables; results of this analysis are detailed in the supplementary material.

Results

NHEJ repair genes are expressed in muscle stem cells and their committed progeny

Given that repair of radiation-induced DSBs in quiescent cells appears to occur primarily by NHEJ (Mohrin, et al., 2010; Sotiropoulou, et al., 2010), to identify the genes responsible for NHEJ repair in the muscle lineage and whether their expression is activated upon DNA damage, *in vitro* irradiated satellite cells were isolated and compared to myoblasts and differentiated myotubes (Fig. 1A). Transgenic *Tg:Pax7-nGFP* mice permit the isolation of satellite cells by FACS after muscle dissociation (Sambasivan et al., 2009). Key regulators of NHEJ following irradiation include Ku70, Ku80, XRCC4, DNA-PKcs, DNA Ligase4, XRCC4-like factor (XLF/Cernunnos), and Artemis (Wyman and Kanaar, 2006). RT-qPCR of the DNA damage repair (DDR) genes showed that, in spite of their metabolically quiescent state, muscle stem cells transcribe all of the known NHEJ genes (Fig. 1B). Satellite cells and myofibre nuclei do not divide, and they are therefore expected to rely essentially on NHEJ to repair DSBs. The first division of satellite cells occurs about 20-30h following injury

(Rocheteau et al., 2012), therefore they were not expected to divide under the conditions tested. At 3h post-IR, NHEJ factors were transcribed at comparable levels as in cultured cells also in satellite cells freshly isolated from irradiated mice (or non-irradiated controls) (Supplementary Fig. S1). Western blot showed lower levels of key NHEJ factors in satellite cells and myoblasts compared to differentiated myotubes (Fig. 1C).

Conversely, proliferating myoblasts, which are expected to rely largely on HR for the repair of DSBs expressed higher levels of the HR factor Rad51 compared to satellite cells and myotubes (Fig. 1D). This result was confirmed by Western blot (Fig. 1E). In addition to HR factors, myoblasts in culture, but not myoblasts isolated from injured mice (either irradiated or not), transcribed key NHEJ factors as non-dividing cells, with protein levels comparable to satellite cells (Fig. 1B and Supplementary Fig. S1). In summary, satellite cells and myoblasts display similarly low levels of NHEJ proteins compared to mytotubes, and satellite cells also express HR factors. We note that ionizing radiation *per se* did not promote significant changes in the transcription of the NHEJ genes tested. Therefore, satellite cells and their progeny express NHEJ factors even in the absence of genotoxic stimulus, suggesting that they are proficient in NHEJ.

Muscle stem cells do not undergo significant apoptosis and retain their differentiation potential after IR-induced genotoxic stress

To investigate the effect of IR-induced genotoxic stress on muscle stem cells, we examined several cellular responses including apoptosis, senescence and differentiation. *Tg:Pax7-nGFP* mice were irradiated with either 5 or 20 Gy, and cells isolated by FACS were used to assess the stem cell response to IR. FACS profiles of total muscle cells enriched for the GFP^+ population and stained with propidium iodide (PI) revealed that 60h post-IR, PI-positive GFP^+ cells accounted for 5.46±0.58% (5 Gy) and 11.17±0.66% (20 Gy) of the GFP^+ population

(Fig. 2A), indicating a good survival of satellite cells even at high IR doses. These values were significantly lower than apoptosis detected upon irradiation of myogenic cells in culture (Caiozzo et al., 2010); however in the latter study, the myogenic cells were isolated by selective growth in culture. Subsequent staining of satellite cells with AnnexinV, a marker of apoptosis (Creutz, 1992) revealed low levels of apoptosis in the GFP^+ population of IR-treated mice compared to control non-irradiated mice. Notably, more apoptotic cells were observed in 20 Gy compared with 5 Gy IR and control mice, albeit in all cases over 90% of the cells were AnnexinV-negative (Fig. 2B). Apoptosis was also measured globally on cells extracted from muscle tissue, which includes a small fraction of satellite cells and a large fraction of differentiated and non-myogenic cells. For this, cells extracted from the muscle were stained with the mitochondrial marker JC1, which provides an early indication of the initiation of cellular apoptosis(Salvioli et al., 1997). A significant number of total cells undergo apoptosis post-IR (Fig. 2C). Thus, the relatively high survival rate and low apoptosis of satellite cells following irradiation is surprising given that cells from the total muscle extract displayed a large apoptotic response. Low levels of apoptosis (<2%) were confirmed 24h post-IR (5 Gy) in satellite cells on cryosections of the *Tibialis anterior* (TA) muscle from irradiated *Tg:Pax7-nGFP* mice (not shown), as well as in satellite cells isolated from irradiated mice (not shown), and immunostained with anti-cleaved Caspase-3.

An analysis of the anti-apoptotic (*Bcl2*, *Bcl-xL*) and proapoptotic (*Bax*, *Bak*) genes (Cory et al., 2003) showed marked differences in their expression among muscle stem cells and their committed progeny (Fig. 2D). Notably, *Bcl2* was expressed the highest in satellite cells, in spite of high levels of its negative regulator *p53* (Mirzayans et al., 2012) and of the p53-target gene and *Bcl2*-antagonist *Bax*. Interestingly, satellite cells also displayed a proapoptotic signature compared to differentiated myotubes, where low levels of expression of *Bcl-xL* and high levels of *Bax* were also observed, which promote alternative complexes with

cytoplasmic p53 to block or promote, respectively, apoptosis (Chipuk et al., 2005). This pro-apoptotic signature may be linked to the distinct basal expression of p53 in satellite cells (Fig. 2D), confirmed by immunofluorescence (Supplementary Fig. S2A). Indeed p53, a mediator of DNA repair, growth arrest, and apoptosis (Kruse and Gu, 2009), is also a key regulator of muscle stem cells number (Schwarzkopf et al., 2006). Interestingly, transient increased levels of p53 upon irradiation was observed by immunofluorescence in satellite cells, indicating that the protein is stabilized in these cells after genotoxic stress, whereas p53 levels remained lower in differentiated myonuclei.

We then determined whether IR affected satellite cell motility and proliferation. Live videomicroscopy showed comparable cell motility and proliferation of irradiated satellite cells compared to control cells (data not shown). Moreover, the number of differentiated cells determined by immunofluorescence with the upstream marker Pax7 and the differentiation marker Myogenin showed rare Myogenin$^+$ cells (<3%) on freshly isolated myofibres from irradiated mice (3x 5 Gy) and non-irradiated controls (Fig. 2E, left panels). These data suggest that differentiation is not a major response to IR for muscle stem cells. In contrast, the number of Pax7$^+$ satellite cells decreased post-IR (Fig. 2E, right upper panel); however, at lower doses (5 Gy; 3x 2 Gy), the number of satellite cells/fibre was not affected, Supplementary Fig. S2B). Cell division, differentiation (Myogenin$^+$) and self-renewal (Pax7$^+$) were maintained also in isolated myofibres irradiated *in vitro* and incubated in culture (Zammit et al., 2004) (Fig. 2E, right lower panel; data not shown). Accordingly, newly formed myoblasts and differentiated myotubes were observed 3-7 days after plating of muscle stem cell isolated from irradiated mice (Supplementary Fig. S2C; data not shown). Once normalized to the original number of cells/fibre, after 72h *ex vivo* Pax7$^+$ cells increased in number by 7.4-fold when originated from non-irradiated mice and 3.8-fold from irradiated mice, suggesting long-term decrease in satellite cell renewal potential after irradiation *in vivo*.

Further, twice as many Myogenin$^+$ differentiated cells were obtained from non-irradiated mice compared to those obtained from irradiated mice. Thus, irradiation *in vivo* and *in vitro* affects satellite cell number and differentiation potential post-IR.

Occurrence of DNA damage and its repair in myogenic cells shortly after irradiation

The presence of DNA damage in the muscle was assessed on cryosections of the TA muscle from irradiated *Tg:Pax7-nGFP* mice, and immunostained with anti-γH2AX (Fig. 3A, upper panel). Histone H2AX is phosphorylated at S139 (γH2AX) in the presence of DSBs, and is used as a general marker of DSBs (Rogakou et al., 1998). Cells were divided into subpopulations according to the number of foci/cell (Fig. 3A, lower panels). Fig. 3B shows that 30 min post-IR the large majority of satellite cells and differentiated myonuclei contained >30 foci indicating extensive and comparable levels of DNA damage in both cell states. However, 2h post-IR satellite cells had less foci/cell compared to differentiated myonuclei, suggesting that the repair of DSBs was faster in the former. Moreover, using single-cell electrophoresis (Fig. 3C) in neutral conditions, we assessed the occurrence of DSBs. Freshly isolated satellite cells and myoblasts (from injured mice) showed similarly high levels of DNA damage immediately after IR, as measured by comet tail moment (Fig. 3D). Moreover, following overnight plating, satellite cells displayed lower levels of DNA damage than myoblasts 6h post-IR, indicating faster repair during this period (Fig. 3E). By 24h, however, myoblasts had also repaired DNA damage as much as satellite cells. Further, in cells isolated by FACS after irradiation *in vivo*, 2h after irradiation the extent of DNA damage measured by comet tail moment and olive moment was lower in satellite cells than in myoblasts (Fig. 3F). Therefore, both electrophoresis of single cells and assessment of DSBs in muscle sections *in vivo* indicate similar levels of DNA damage upon irradiation in satellite vs. myoblasts or differentiated cells, and suggest a more rapid repair of DSBs in satellite cells than in myoblasts or differentiated myonuclei.

By immunofluorescence of pATM (phosphoS1981), we also observed activated DNA damage response in satellite cells and differentiated myonyuclei within the myofibre upon irradiation (Supplementary Fig. S3B). We then assessed the efficiency and kinetics of DSB repair in satellite cells, using high-resolution imaging and statistical analysis of DSB nuclear markers in single cells (Chayot, Danckaert, et al., 2010). Enumeration of γH2AX and 53BP1 (a DDR factor that is retained at DSBs) foci loss by immunofluorescence has been successfully employed to measure DSB repair upon genotoxic stress (Noon et al., 2010). We found that at short time post-IR satellite cells displayed robust DSB repair either as isolated cells or within the myofibre (Supplementary Fig. S3A,D). As γH2AX is not fully specific for DSB (Marti et al., 2006) and is also sensitive to chromosomal environment (Seo et al., 2012) for the next experiments we used 53BP1 as DSB immunomarker.

Isolated muscle stem cells repair IR-induced DSB more efficiently than their differentiated progeny

We tested DSB repair at longer times post-IR, under conditions compatible with all experimental systems used in this study (see next sections), and where differences in repair kinetics were assessed by enumeration using DSB markers. In the first of three experimental paradigms, the kinetics of DSB repair was determined in freshly isolated satellite cells, myoblasts (cultured for 3 days), and myotubes (cultured for 10-11 days). Although non-irradiated control cells showed little to no 53BP1 foci (~1-3/nucleus), all cell states examined exhibited between 10-15 nuclear foci 3h after 5 Gy IR (Fig. 4). Interestingly, at 3h and 6h after IR, satellite cells had significantly fewer 53BP1 foci compared to myoblasts and myotubes (n=3 animals). In addition, the decline in number of foci was greater in satellite cells than in myoblasts and in myotubes. By 24h all cells retained some unrepaired DNA damage, indicating persistence of DNA damage, however in satellite cells and myoblasts this number was slightly higher than background levels, whereas 3.4±0.2 foci persisted in

myotubes.

These observations indicate that muscle stem cells repair radiation-induced DSBs more efficiently than their committed progeny in culture. They also show that proliferating cells repair DSBs less rapidly than quiescent cells. Moreover, the absence of proliferation is associated with either high or low repair efficiency (satellite cells and myotubes, respectively), suggesting that the proliferation state might not be the major determinant in the efficiency of DSB repair.

Muscle stem cells repair IR-induced DSB more efficiently than their differentiated progeny in myofibres *in vitro* and *in vivo*.

Next we investigated DSB repair on isolated myofibres where muscle stem cells remain associated with their niche and where the quiescent and differentiated states reflect cell cycle exit at the time of isolation. We showed that at short times post-IR γH2AX signal decreases more rapidly in satellite cells than in differentiated cells (see Supplementary Fig. S3C,D). Fig. 5 shows that at longer intervals post-IR (3h-24h), proliferating myoblasts repair radiation-induced DNA damage less efficiently than quiescent satellite cells, however both repair more efficiently than differentiated cells *in vitro,* confirming results in isolated cells in culture. Although satellite cells maintained a high efficiency of repair either as isolated cells or in their niche, differences appeared more dramatic in myofibres and myoblasts compared to their *ex vivo* counterparts.

These results were confirmed in fibres and myoblasts isolated from mice irradiated *in vivo* (Supplementary Fig. S4), including after multiple irradiation (Supplementary Fig. S5).

Although in all tested conditions the reduction of DSB-related markers post-IR was more efficient in satellite cells than in myoblasts and in differentiated cells, a few differences were noted. Myoblasts displayed similar repair kinetics under all tested conditions (middle panel,

Supplementary Fig. S6). Conversely, satellite cells in fibres appeared to repair more efficiently than isolated satellite cells at least in the first 6h post-IR, although they retained slightly higher levels of residual damage at 24h post-IR (left panel). Differentiated cells displayed higher numbers of residual DSBs within the myofibre than in culture (right panel). In all cases, the kinetics of DSB-related foci was not significantly altered whether irradiation and repair took place *in vivo* or *in vitro*. Thus, the niche appears to have a minor impact on the repair of IR-induced DNA damage in satellite cells.

Efficient and accurate repair of DSB substrates by NHEJ in satellite cells

Reporter plasmids are then used to assay NHEJ in living cells (Sotiropoulou, et al., 2010). Recently, we developed a method to assess the frequency of NHEJ using a highly sensitive plasmid-based assay that correlates robustly with repair on the chromosome, and allows enumerating the efficiency of DSB repair (Fig. 6A)(Chayot, Montagne, et al., 2010; Chayot et al., 2012). Fig. 6B shows that the repair efficiency was at least as high or higher in satellite cells ($f=10^{-3}$) compared to MEFs ($f=5 \times 10^{-5}$; as in previous report (Chayot, et al., 2012)). Importantly, a 90% reduction of NHEJ was observed in satellite cells in the presence of a specific inhibitor of DNA-PKcs (NU 7441 (Leahy et al., 2004)), which is a major mediator of NHEJ, compared to the controls (Fig. 6C), indicating that DNA-PKcs plays a crucial role in the repair of NHEJ substrates in satellite cells.

Sequencing and restriction digestion identified accurate repair events (Supplementary Fig. S7). We observed that satellite cells exhibited a strikingly more accurate repair of DSBs compared to MEFs ($4.8\pm0.2 \times 10^{-4}$, and $2.2\pm0.4 \times 10^{-5}$, respectively; the latter confirming previous findings (Chayot, et al., 2012)), (Fig. 6D). Sequencing also revealed that inaccurate events consisted of either large deletions (>30bp) or micromodifications (1-10 nucleotides) in similar proportions (not shown). Most deletions rely on microhomology (1-6 nucleotides, a

hallmark of alternative-NHEJ compared to the more accurate classical-NHEJ (Nussenzweig and Nussenzweig, 2007) (Fig. 6F-G). Notably, in satellite cells accurate events depend on classical NHEJ, since the frequency of these events dropped to 10% in the presence of the NHEJ inhibitor, whereas inaccurate events were minimally affected (micromodifications) or unaffected (deletions) (Fig. 6E). In contrast, in MEFs, accurate and inaccurate repair events were reduced in the presence of the NHEJ inhibitor. Compared to satellite cells and MEFs, myoblasts displayed highly variable repair efficiencies and accuracies, probably reflecting a larger sensitivity to experimental conditions and heterogeneities reflecting different levels of commitment, and they repaired either accurately or through large or small deletions, in the presence and in the absence of microhomology (not shown). These results indicate that the repair of NHEJ-substrates is not only more efficient, but also more accurate in satellite cells compared to fibroblasts, and that accurate events essentially depend on classical NHEJ, where DNA-PKcs plays a major role.

Discussion

Genotoxic stress and DNA damage are considered to be major causes of aging in mammals. The risk of mutation load and loss of genome integrity in adult stem cells has been proposed to be the principal cause of age related decline in tissue function (Ruzankina, et al., 2008). Here we show that muscle stem cells repair DSBs significantly more efficiently than their committed progeny. Satellite cells are quiescent, and they repair much more efficiently than post-mitotic differentiated myonuclei, raising the question whether reversible and irreversible cell cycle exit, affects repair efficiency. Interestingly, the stem cells retain this capacity independent of the niche. Although the repair efficiency varies slightly in different experimental conditions, satellite cells systematically repair IR-induced DNA damage more efficiently than their progeny under similar conditions. In addition, we show that NHEJ is a major mediator of this mechanism and that it operates with unexpected accuracy on DSB

substrates. Notably, the efficiency of repair decreases as a function of cell differentiation, whereas the proliferation state *per se* is not a major determinant. These findings provide important information on how stem cells maintain genome integrity, and they could be extended to other systems, including cancer stem cells.

The fate of muscle stem cells in response to IR-induced genotoxic stress

High doses of limb irradiation, 18-25 Gy (Boldrin, et al., 2012; Gross and Morgan, 1999; Heslop, et al., 2000), result in the loss of the majority of muscle stem cells, and failure of the remaining cells to undergo mitosis resulting in loss of regenerative capacity. In agreement with these findings, we showed that a fractionated 15 Gy total body irradiation regime reduced the stem cell numbers after 22 days. Lower IR doses (5 Gy; fractionated 6 Gy), at shorter times post-IR, did not result in depletion of satellite cells. Interestingly, up to 15% of stem cell progeny undergo cellular senescence in culture post-IR. It is not clear if this is also the case *in vivo* where cell clearing mechanisms, such as macrophage-dependent phagocytosis, could limit this analysis. Thus, even the highest doses of IR tested here were not sufficient to significantly compromise the function of the surviving muscle stem cells, in agreement with the cited reports.

Muscle stem cells display robust survival to 20 Gy of total body irradiation where about 90% resist to apoptosis whilst up to two thirds of cells in the total muscle tissue undergo apoptosis. Further, less than 70% of differentiated MEFs survive after 5 Gy IR (Chayot, et al., 2010). These data are compatible with muscle regeneration observed after 18 Gy irradiation (Boldrin, et al., 2012). The striking resistance of muscle stem cells to apoptosis following DNA damage is compatible with the observed high expression levels of antiapoptotic *Bcl2* compared to myoblasts and differentiated cells. This was also the case for Bcl2-dependent antiapototic response of hair-follicle-bulge stem cells compared to non-bulge cells (Sotiropoulou, et al., 2010), whereas *Bcl2* is not expressed at higher levels in HSPCs compared to myeloid

progenitors (Mohrin, et al., 2010). Notably the expression of *p53* and of p53-target genes (including proapoptotic *Bax*) does not increase after irradiation of muscle stem cells. These observations suggest that in the presence of high levels of p53 and apoptotic genes, the anti-apoptotic response may be mediated by robust expression of *Bcl-2*. These findings also reveal that the relative resistance to apoptosis after DNA damage is differently regulated by members of the Bcl2 family in distinct types of stem cells.

Highly accurate repair of DSB substrates in stem cells

Two factors could seriously affect the fate of irradiated cells: persistence of unrepaired DNA damage and inaccuracy of repair. Unrepaired DNA damage post-IR is a potential threat for cycling cells where checkpoints arrest the cell cycle until repair is effected, or cells undergo apoptosis. Persistent DNA damage can also trigger inaccurate repair, as is the case in NHEJ mutants (Nussenzweig and Nussenzweig, 2007). We observed that not only quiescent muscle stem cells but also proliferating myoblasts retain a low number of persistent 53BP1 foci/cell at 24h post-IR, in all tested conditions. These findings indicate that myoblasts are able to recover within hours, whereas differentiated myonuclei are not. Nevertheless, proliferating muscle stem cells do not display better repair efficiency than satellite cells, in spite of the expression of classical-NHEJ genes at least as much as in satellite cells, and higher levels of Rad51, a key effector of HR. Conversely, mobilized and pre-cultured HSPCs were reported to retain a lower number of persistent 53BP1 foci than quiescent HSPCs, compatible with the activation of recombination-dependent repair (Mohrin, et al., 2010).

In the absence of irradiation, proliferating myoblasts were reported to display up to 2-fold more γH2AX-positive cells than quiescent muscle stem cells (Cousin et al., 2013). This labeling is compatible with replication-induced DNA damage (Branzei and Foiani, 2010), for 53BP1 labelling (Lukas et al., 2011), and for genome-wide γH2AX enrichment in cycling

versus resting cells in the absence of IR (Seo, et al., 2012). Therefore, proliferating muscle stem cells undergo a larger number of endogenous DNA damage events compared to quiescent cells, as expected for cycling cells, rather than showing selective accumulation of DNA damage.

A major finding from the present study is that muscle stem cells repair DSBs with high efficiently and accuracy. Accurate repair of these substrates in the stem cells is dependent on the key classical-NHEJ factor DNA-PKcs, which promotes synapsis of the DNA ends and activates other components of the repair machinery (Dobbs et al., 2010). The inhibition of DNA-PKcs specifically drops accurate events by about 10-fold. This capacity of the stem cells to perform accurate repair differs markedly with that of HSPCs where significant genomic rearrangements were observed (Mohrin, et al., 2010).

Radiation-resistance and DNA repair efficiency

Regeneration is a multifactorial process that involves multiple cell types and a functional niche (Boldrin, et al., 2012; Saclier, et al., 2013; Yin et al., 2013). The niche might not have protective properties for highly doses of strongly penetrating IR used here (Reisz et al., 2014), as it appears to be for endogenous oxidative stress (Pallafacchina et al., 2010). Interestingly, thrombopoietin a factor of the hematopoietic niche, has been shown to stimulate DNAPKcs-dependent repair in HSPCs (de Laval et al., 2013). The repair efficiency of muscle stem cells was reported to remain high, at least for replication-induced DSBs, in aged animals (Cousin, et al., 2013), underscoring the robustness of DNA damage response in these cells. However, regeneration capacity has been reported to decline with age (Gopinath and Rando, 2008). In agreement with this notion, quiescent, but not activated muscle stem cells from old mice display lower regeneration potential than those from young mice after high doses of irradiation (Cousin, et al., 2013).

Colony formation of myogenic cells from mice with impaired DSB repair (SCID mice) was reported to be lower than in normal mice, suggesting that DNA damage repair plays a role in myoblast expansion in culture (Cousin, et al., 2013). These authors also reported that in the absence of irradiation, regeneration efficiency was comparable in SCID and control mice, leading to the suggestion that DNA DSB repair deficiency does not impact regeneration capacity during ageing. However, it is well established that the immune response, including infiltrate and macrophages, plays a critical role in the regeneration outcome (Saclier, Cuvellier, et al., 2013). Further, the absence of T and B cells in SCID mice improves muscle regeneration due to diminution of pro-inflammatory macrophages (Farini et al., 2012), independently of DNA damage repair. Thus, the SCID model compromises the immune response and NHEJ, but not homologous recombination. To resolve these issues, a model that affects only DSB response, while maintaining the immune response, should be examined. This underscores the importance of initiating a systematic analysis of each cell type following irradiation induced DNA damage, as we have done for myogenic cells in the present study. Our data and recent findings on the accumulation of DNA damage-induced chromatin alterations in hair-follicle stem cells (Schuler and Rube, 2013), are compatible with the notion that DNA damage plays a role in stem cell ageing.

How cell differentiation affects DSB repair remains an open question. It would be interesting to determine if depletion of the stem cell pool after irradiation is random, or whether subpopulations are more resistant (Kuang et al., 2007; Rocheteau, et al., 2012; Shinin et al., 2006; Tajbakhsh, 2009) and if muscle stem cells use the same repair pathways compared to their committed progeny.

Acknowledgements

We thank Laurent Chatre, Barbara Gayraud-Morel, Ewa Kotula, Ramkumar Sambasivan for their assistance, members of the MR and ST laboratories for helpful discussions, and Imagopole (PFID) for advice. This work was supported by Institut Pasteur, Centre National de la Recherche Scientifique, EU Framework 7 project EuroSysStem, Electricité de France Radioprotection, Association Recherche sur le Cancer/Institut National du Cancer, Agence Nationale de la Recherche.

Nonstandard abbreviations

DDR	DNA damage repair
DMSO	dimethyl sulfoxide
DMEM	Dulbecco's modified Eagle medium
DSB	double-strand break
EDL	*extensor digitorum longus*
FCS	foetal calf serum
FACS	fluorescence activated cell sorting
GFP	green fluorescent protein
HR	homologous recombination
HSPCs	hematopoietic stem and progenitor cells
IR	ionizing radiation
MEFs	mouse embryonic fibroblasts
MPs	myeloid progenotors
NHEJ	non-homologous end-joining
PBS	phosphate buffered saline
PFA	paraformaldheyde
PI	propidium iodide
RT-qPCR	real time quantitive PCR
SCID	severe combined immunodeficiency
TA	*Tibialis anterior*

References

Blanpain, C., Mohrin, M., Sotiropoulou, P. A., and Passegue, E. (2011). DNA-damage response in tissue-specific and cancer stem cells. Cell Stem Cell, *8*, 16-29.

Boldrin, L., Neal, A., Zammit, P. S., Muntoni, F., and Morgan, J. E. (2012). Donor satellite cell engraftment is significantly augmented when the host niche is preserved and endogenous satellite cells are incapacitated. Stem Cells, *30*, 1971-1984.

Branzei, D., and Foiani, M. (2010). Maintaining genome stability at the replication fork. Nat Rev Mol Cell Biol, *11*, 208-219.

Caiozzo, V. J., Giedzinski, E., Baker, M., et al. (2010). The radiosensitivity of satellite cells: cell cycle regulation, apoptosis and oxidative stress. Radiat Res, *174*, 582-589.

Chapman, J. R., Taylor, M. R., and Boulton, S. J. (2012). Playing the end game: DNA double-strand break repair pathway choice. Mol Cell, *47*, 497-510.

Chayot, R., Danckaert, A., Montagne, B., and Ricchetti, M. (2010). Lack of DNA polymerase mu affects the kinetics of DNA double-strand break repair and impacts on cellular senescence. DNA Repair (Amst), *9*, 1187-1199.

Chayot, R., Montagne, B., Mazel, D., and Ricchetti, M. (2010). An end-joining repair mechanism in Escherichia coli. Proc Natl Acad Sci U S A, *107*, 2141-2146.

Chayot, R., Montagne, B., and Ricchetti, M. (2012). DNA polymerase mu is a global player in the repair of non-homologous end-joining substrates. DNA Repair (Amst), *11*, 22-34.

Chipuk, J. E., Bouchier-Hayes, L., Kuwana, T., Newmeyer, D. D., and Green, D. R. (2005). PUMA couples the nuclear and cytoplasmic proapoptotic function of p53. Science, *309*, 1732-1735.

Cory, S., Huang, D. C., and Adams, J. M. (2003). The Bcl-2 family: roles in cell survival and oncogenesis. Oncogene, *22*, 8590-8607.

Cousin, W., Ho, M. L., Desai, R., et al. (2013). Regenerative Capacity of Old Muscle Stem Cells Declines without Significant Accumulation of DNA Damage. PLoS One, *8*, e63528.

Creutz, C. E. (1992). The annexins and exocytosis. Science, *258*, 924-931.

de Laval, B., Pawlikowska, P., Petit-Cocault, L., et al. (2013). Thrombopoietin-increased DNA-PK-dependent DNA repair limits hematopoietic stem and progenitor cell mutagenesis in response to DNA damage. Cell Stem Cell, *12*, 37-48.

Dobbs, T. A., Tainer, J. A., and Lees-Miller, S. P. (2010). A structural model for regulation of NHEJ by DNA-PKcs autophosphorylation. DNA Repair (Amst), *9*, 1307-1314.

Farini, A., Sitzia, C., Navarro, C., et al. (2012). Absence of T and B lymphocytes modulates dystrophic features in dysferlin deficient animal model. Exp Cell Res, *318*, 1160-1174.

Gayraud-Morel, B., Chretien, F., Flamant, P., Gomes, D., Zammit, P. S., and Tajbakhsh, S. (2007). A role for the myogenic determination gene Myf5 in adult regenerative myogenesis. Dev Biol, *312*, 13-28.

Gayraud-Morel, B., Chretien, F., Jory, A., et al. (2012). Myf5 haploinsufficiency reveals distinct cell fate potentials for adult skeletal muscle stem cells. J Cell Sci, *125*, 1738-1749.

Gayraud-Morel, B., Chretien, F., and Tajbakhsh, S. (2009). Skeletal muscle as a paradigm for regenerative biology and medicine. Regen Med, *4*, 293-319.

Gopinath, S. D., and Rando, T. A. (2008). Aging of the Skeletal Muscle Stem Cell Niche. Aging Cell.

Gross, J. G., and Morgan, J. E. (1999). Muscle precursor cells injected into irradiated mdx mouse muscle persist after serial injury. Muscle Nerve, *22*, 174-185.

Heslop, L., Morgan, J. E., and Partridge, T. A. (2000). Evidence for a myogenic stem cell that is exhausted in dystrophic muscle. J Cell Sci, *113 (Pt 12)*, 2299-2308.

Hua, G., Thin, T. H., Feldman, R., et al. (2012). Crypt base columnar stem cells in small intestines of mice are radioresistant. Gastroenterology, *143*, 1266-1276.

Inomata, K., Aoto, T., Binh, N. T., et al. (2009). Genotoxic stress abrogates renewal of melanocyte stem cells by triggering their differentiation. Cell, *137*, 1088-1099.

Jory, A., Le Roux, I., Gayraud-Morel, B., et al. (2009). Numb promotes an increase in skeletal muscle progenitor cells in the embryonic somite. Stem Cells, *27*, 2769-2780.

Kruse, J. P., and Gu, W. (2009). Modes of p53 regulation. Cell, *137*, 609-622.

Kuang, S., Kuroda, K., Le Grand, F., and Rudnicki, M. A. (2007). Asymmetric self-renewal and commitment of satellite stem cells in muscle. Cell, *129*, 999-1010.

Leahy, J. J., Golding, B. T., Griffin, R. J., et al. (2004). Identification of a highly potent and selective DNA-dependent protein kinase (DNA-PK) inhibitor (NU7441) by screening of chromenone libraries. Bioorg Med Chem Lett, *14*, 6083-6087.

Li, L., and Clevers, H. (2010). Coexistence of quiescent and active adult stem cells in mammals. Science, *327*, 542-545.

Lombard, D. B., Chua, K. F., Mostoslavsky, R., Franco, S., Gostissa, M., and Alt, F. W. (2005). DNA repair, genome stability, and aging. Cell, *120*, 497-512.

Lukas, C., Savic, V., Bekker-Jensen, S., et al. (2011). 53BP1 nuclear bodies form around DNA lesions generated by mitotic transmission of chromosomes under replication stress. Nat Cell Biol, *13*, 243-253.

Marti, T. M., Hefner, E., Feeney, L., Natale, V., and Cleaver, J. E. (2006). H2AX phosphorylation within the G1 phase after UV irradiation depends on nucleotide excision repair and not DNA double-strand breaks. Proc Natl Acad Sci U S A, *103*, 9891-9896.

Mirzayans, R., Andrais, B., Scott, A., and Murray, D. (2012). New insights into p53 signaling and cancer cell response to DNA damage: implications for cancer therapy. J Biomed Biotechnol, *2012*, 170325.

Mohrin, M., Bourke, E., Alexander, D., et al. (2010). Hematopoietic stem cell quiescence promotes error-prone DNA repair and mutagenesis. Cell Stem Cell, *7*, 174-185.

Nijnik, A., Woodbine, L., Marchetti, C., et al. (2007). DNA repair is limiting for haematopoietic stem cells during ageing. Nature, *447*, 686-690.

Noon, A. T., Shibata, A., Rief, N., et al. (2010). 53BP1-dependent robust localized KAP-1 phosphorylation is essential for heterochromatic DNA double-strand break repair. Nat Cell Biol, *12*, 177-184.

Nussenzweig, A., and Nussenzweig, M. C. (2007). A backup DNA repair pathway moves to the forefront. Cell, *131*, 223-225.

Olive, P. L., and Banath, J. P. (2006). The comet assay: a method to measure DNA damage in individual cells. Nat Protoc, *1*, 23-29.

Pagel, C. N., and Partridge, T. A. (1999). Covert persistence of mdx mouse myopathy is revealed by acute and chronic effects of irradiation. J Neurol Sci, *164*, 103-116.

Pallafacchina, G., Francois, S., Regnault, B., et al. (2010). An adult tissue-specific stem cell in its niche: a gene profiling analysis of in vivo quiescent and activated muscle satellite cells. Stem Cell Res, *4*, 77-91.

Potten, C. S., Gandara, R., Mahida, Y. R., Loeffler, M., and Wright, N. A. (2009). The stem cells of small intestinal crypts: where are they? Cell Prolif, *42*, 731-750.

Reisz, J. A., Bansal, N., Qian, J., Zhao, W., and Furdui, C. M. (2014). Effects of ionizing radiation on biological molecules-mechanisms of damage and emerging methods of detection. Antioxid Redox Signal, *21*, 260-292.

Relaix, F., and Zammit, P. S. (2012). Satellite cells are essential for skeletal muscle regeneration: the cell on the edge returns centre stage. Development, *139*, 2845-2856.

Reya, T., Morrison, S. J., Clarke, M. F., and Weissman, I. L. (2001). Stem cells, cancer, and cancer stem cells. Nature, *414*, 105-111.

Rocheteau, P., Gayraud-Morel, B., Siegl-Cachedenier, I., Blasco, M. A., and Tajbakhsh, S. (2012). A subpopulation of adult skeletal muscle stem cells retains all template DNA strands after cell division. Cell, *148*, 112-125.

Rogakou, E. P., Pilch, D. R., Orr, A. H., Ivanova, V. S., and Bonner, W. M. (1998). DNA double-stranded breaks induce histone H2AX phosphorylation on serine 139. J Biol Chem, *273*, 5858-5868.

Rossi, D. J., Bryder, D., Seita, J., Nussenzweig, A., Hoeijmakers, J., and Weissman, I. L. (2007). Deficiencies in DNA damage repair limit the function of haematopoietic stem cells with age. Nature, *447*, 725-729.

Rothkamm, K., and Lobrich, M. (2003). Evidence for a lack of DNA double-strand break repair in human cells exposed to very low x-ray doses. Proc Natl Acad Sci U S A, *100*, 5057-5062.

Ruzankina, Y., Asare, A., and Brown, E. J. (2008). Replicative stress, stem cells and aging. Mech Ageing Dev, *129*, 460-466.

Saclier, M., Cuvellier, S., Magnan, M., Mounier, R., and Chazaud, B. (2013). Monocyte/macrophage interactions with myogenic precursor cells during skeletal muscle regeneration. FEBS J.

Saclier, M., Yacoub-Youssef, H., Mackey, A. L., et al. (2013). Differentially activated macrophages orchestrate myogenic precursor cell fate during human skeletal muscle regeneration. Stem Cells, *31*, 384-396.

Salvioli, S., Ardizzoni, A., Franceschi, C., and Cossarizza, A. (1997). JC-1, but not DiOC6(3) or rhodamine 123, is a reliable fluorescent probe to assess delta psi changes in intact cells: implications for studies on mitochondrial functionality during apoptosis. FEBS Lett, *411*, 77-82.

Sambasivan, R., Gayraud-Morel, B., Dumas, G., et al. (2009). Distinct regulatory cascades govern extraocular and pharyngeal arch muscle progenitor cell fates. Dev Cell, *16*, 810-821.

Schuler, N., and Rube, C. E. (2013). Accumulation of DNA damage-induced chromatin alterations in tissue-specific stem cells: the driving force of aging? PLoS One, *8*, e63932.

Schwarzkopf, M., Coletti, D., Sassoon, D., and Marazzi, G. (2006). Muscle cachexia is regulated by a p53-PW1/Peg3-dependent pathway. Genes Dev, *20*, 3440-3452.

Seo, J., Kim, S. C., Lee, H. S., et al. (2012). Genome-wide profiles of H2AX and gamma-H2AX differentiate endogenous and exogenous DNA damage hotspots in human cells. Nucleic Acids Res, *40*, 5965-5974.

Shinin, V., Gayraud-Morel, B., Gomes, D., and Tajbakhsh, S. (2006). Asymmetric division and cosegregation of template DNA strands in adult muscle satellite cells. Nat Cell Biol, *8*, 677-687.

Smith, J., Baldeyron, C., De Oliveira, I., Sala-Trepat, M., and Papadopoulo, D. (2001). The influence of DNA double-strand break structure on end-joining in human cells. Nucleic Acids Res, *29*, 4783-4792.

Sotiropoulou, P. A., Candi, A., Mascre, G., et al. (2010). Bcl-2 and accelerated DNA repair mediates resistance of hair follicle bulge stem cells to DNA-damage-induced cell death. Nat Cell Biol, *12*, 572-582.

Tajbakhsh, S. (2009). Skeletal muscle stem cells in developmental versus regenerative myogenesis. J Intern Med, *266*, 372-389.

Wakeford, S., Watt, D. J., and Partridge, T. A. (1991). X-irradiation improves mdx mouse muscle as a model of myofiber loss in DMD. Muscle Nerve, *14*, 42-50.

Wyman, C., and Kanaar, R. (2006). DNA double-strand break repair: all's well that ends well. Annu Rev Genet, *40*, 363-383.

Yin, H., Price, F., and Rudnicki, M. A. (2013). Satellite cells and the muscle stem cell niche. Physiol Rev, *93*, 23-67.

Zammit, P. S., Golding, J. P., Nagata, Y., Hudon, V., Partridge, T. A., and Beauchamp, J. R. (2004). Muscle satellite cells adopt divergent fates: a mechanism for self-renewal? J Cell Biol, *166*, 347-357.

Zammit, P. S., Partridge, T. A., and Yablonka-Reuveni, Z. (2006). The skeletal muscle satellite cell: the stem cell that came in from the cold. J Histochem Cytochem, *54*, 1177-1191.

Figure 1. Expression of NHEJ and HR factors in satellite cells and in their progeny. A) Scheme of myogenesis, adapted from (Zammit et al., 2006), indicating key myogenic markers and replicative state of cells. **B)** RT-qPCR of NHEJ genes. Satellite cells were isolated by FACS from *Tg:Pax7-nGFP* mice and assayed directly (overnight seeding) or cultured to give rise to myoblasts in culture (3 days) and myotubes (10-11 days), n=3 (myoblasts and myotubes) or n=5 (satellite cells) mice/condition. Cells were irradiated at 5 Gy (1 Gy ≈25-40 DSBs/mammalian cell (Rothkamm and Lobrich, 2003). With the exception of Ligase 4 (Lig4; expressed at higher levels in satellite cells than myotubes), the other NHEJ factors were expressed at higher or at similar levels in both. **C)** Western blots of key NHEJ factors and reference GAPDH in cells treated as in panel B, and also in satellite cells (first two lanes) freshly isolated from irradiated and non-irradiated mice (3h post-IR or non-irradiated). **D)** RT-qPCR of HR genes. **E)** Western blots of the HR factor 53BP1 and reference GAPDH in cells treated as in panel D. See supplementary material for the Two-Way ANOVA analysis. Mean ± SEM; unpaired t tests * $p<0.05$; ** $p<0.01$, *** $p<0.001$.

Figure 2. Evaluation of the cellular response of muscle stem cells to irradiation. A) FACS profiles of control, 5 Gy and 20 Gy IR *Tg:Pax7-nGFP* mice; satellite cells were assayed 60h after IR and compared with non-IR controls (n=3 mice/condition). FACS profiles of total myogenic cells enriched for GFP^+ population and percent of PI-positive GFP^+ cells (mean ± SEM). **B)** GFP^+ cells were assayed for apoptosis (FACS AnnexinV-Alexa568 treated GFP^+ cells, percent Annexin-positive GFP^+; mean ± SD). Red (apoptosis), green (GFP, satellite cells) fluorescence indicated. For AnnexinV control, satellite cells were cultured, treated 4-6h with H_2O_2 (1 mM) to induce apoptosis, and the gate was adjusted for AnnexinV positivity (control: 12.6%; H_2O_2: 87.4%, not shown). **C)** Muscle extracts from control, 5 Gy and 20 Gy irradiated mice (harvested 60h post-IR; see Fig. 2A) were treated with JC-1 (Cayman's JC-1 Mitochondrial Membrane Potential Assay Kit) which measures changes in mitochondrial

membrane potential, Δψm, a critical parameter of mitochondrial function used as an indicator of cell health (healthy cells, red; apoptotic cells, green). Representative plots of *Tg:Pax7-nGFP* mice shown for control, IR 5Gy, and IR 20Gy mice (n=3 mice/condition). Green fluorescence values shown on right panel; mean ± SD. Mann Withney test, *** $p \leq 0.001$. **D)** RT-qPCR of pro-apoptotic and anti-apoptotic genes involved in cell survival. Freshly isolated satellite cells (overnight seeding) compared to cultured myoblasts (3 days) and myotubes (10-11 days); n=4 for satellite cells (but *Bax* n=3) and myotubes; n=3 for myoblasts (but n=2 for 0 Gy 6h) condition. **E)** Wild-type mice were exposed to 3 rounds of 5Gy IR (individual sublethal dose) at two-day intervals and sacrificed after 22 days. Myofibres were stained with anti-Pax7 and anti-Myogenin antibodies (left panels). Satellite cells were enumerated on freshly isolated EDL myofibres stained for Pax7 (top histogram) and Myogenin (<3% positive cells in both conditions, data not shown). Continuous differentiation and fusion with myofibre might occur after IR, however, centrally located myonuclei (hallmark of newly fused cells), were not noted. Unaffected differentiation could be due to satellite cells remaining in niche with unrepaired DSBs, which would then undergo mitotic checkpoint arrest upon activation and enter apoptosis. To test for this, cell division, differentiation ($Myogenin^+$) and self-renewal ($Pax7^+$) were assessed (Zammit, et al., 2004) in niche associated satellite cells from control and irradiated (3 x 5 Gy) mice incubated without attachment for 3 days (right lower panel) and for 4-7 days (Supplementary Fig. S1C; data not shown). IR-treated mice exhibited all of these properties, confirming no change in cell fate upon IR. Unpaired t tests * $p<0.05$; ** $p<0.01$; *** $p<0.001$.

Figure 3. Occurrence of DNA damage in satellite cells, myoblasts and differentiated cells upon irradiation. A) Muscle cross-sections from TA muscle extracted from *Tg:Pax7-nGFP* non-irradiated and irradiated (5Gy) mice 30 min and 2h post-IR. Upper panels, muscle cross-sections immunostained with anti-GFP (for Pax7-GFP), anti-γH2AX, and Hoechst for nuclei.

Anti-GFP and merge panels are intentionally overexposed for the 488-fluorescence to identify the individual myofibres (upper right panel, contour of one myofibre). Arrowhead, satellite cells (Pax7-GFP$^+$); arrow, differentiated nuclei. Lower panels, satellite cells (Pax7-GFP$^+$) and myonuclei (Pax7-GFP$^-$) at higher magnification. Cells from sections at 30 min and 2h post-IR are shown. **B)** Percent of satellite (sat) and differentiated (diff) cells with indicated number of γH2AX foci. Irradiated (n=20 for each time point) and non-irradiated (n=30) satellite cells, and irradiated (n=27 for 30m in, n= 100 for t=2h) and non-irradiated (n= 35) differentiated nuclei were analysed from 8 (no IR) and 16 cross-sections (30 min and 2h), and n=2 mice. **C)** Upper panel: schematic of key parameters for analysis of DSBs by neutral comet assay. **D)** Tail moment of non-irradiated and irradiated satellite cells and myoblasts (from injury) immediately (<5 min) after irradiation (n=3 mice/condition); Mann Withney test. **E)** Tail moment of satellite cells and myoblasts at different time point following IR *in vitro* (n=3 mice/condition) Unpaired t test. **F)** Left panels: Microscopic fluorescent view of freshly isolated satellite cells and myoblasts (from injured mice) irradiated *in vivo* or non-irradiated submitted to an electrophoretic field, 2h post-IR (5 Gy). The schema on the right corresponds to the treatment of either limb in each mouse. Irradiated satellite cells and myoblasts exhibit significant migration of damaged DNA compared to non-irradiated cells, resulting in high values of the comet tail moment and olive moment compared to cells from non-irradiated mice, as expected. Panels on lower right show quantification of Tail moment and Olive moment in all conditions tested (n=300 cells/condition, n=2 mice) Unpaired t test; *** $p<0.001$.

Figure 4. More efficient repair of DSBs in muscle satellite cells than in myoblasts and myotubes in culture. A) Satellite cells were isolated by FACS, plated for 12-14h, exposed to 5Gy IR, or cultured to give rise to **B)** myoblasts in culture (3 days) and **C)** myotubes (10-11 days) then irradiated, and harvested at indicated times post-IR. n=3 mice/condition. Sites of

DSB repair were revealed by anti-53BP1 (red) and nuclei with Hoechst; panels below in C are immune labeled with differentiation marker Myogenin (green). **D)** Enumeration of 53BP1 foci at time intervals after irradiation of satellite cell and committed progeny in culture. Mean ± SEM; unpaired t test (* $p \leq 0.05$, ** $p \leq 0.01$, *** $p \leq 0.001$). Insets, number of foci/nucleus as a function of time post IR. DSB repair kinetics appeared bi-phasic for satellite cells and their progeny, with a more rapid phase before 6h. For satellite cells and myoblasts compare these kinetics with those of residual DNA damage in Fig 3E.

Figure 5. Efficient repair response to IR-induced DSBs in muscle stem cells in the myofibre niche *in vitro*. A) Scheme of *in vitro* experiments. Immunoflourescence (IF). **B)** Freshly isolated EDL myofibres from *Tg:Pax7-nGFP* mice exposed to 5Gy IR; DSB foci were enumerated (n=5 mice) using anti-53BP1 staining. White arrowheads, satellite cells (anti-GFP antibody). **C**) Histogram of number of 53BP1 foci after IR. *Per* condition, 150-200 satellite cells and differentiated myonuclei were counted, from 75 myofibres (n=4 mice). Myoblasts from *Tg:Pax7-nGFP* injured mice were isolated by FACS, irradiated or non-irradiated and fixed at indicated time points (300 cells analysed/condition; n=3 mice). Average number of 53BP1 foci in differentiated myonuclei was significantly higher (3-fold at 3h post-isolation) than in satellite cells. From 3-24h post-IR, satellite cells had an average of 4-7 foci/nucleus; differentiated nuclei had 22 foci/nucleus (n=5 mice). Myoblasts had 72% and 50% more foci than satellite cells at 3h and 6h, respectively. Residual DNA damage was noted at 24h, with satellite cells and FACS-isolated myoblasts from injured mice displaying an average of ≤4 foci/nucleus, whereas differentiated cells in fibres retained more than 10 foci. In absence of irradiation, myoblasts displayed higher background level of 53BP1 foci than other nuclei, probably due to DNA damage produced during DNA replication (Branzei and Foiani, 2010; Lukas, et al., 2011). Myoblast immunolabelling not shown in panel A. Mean ± SEM. Unpaired t test, *** $p<0.001$ Nd, not done. Insets, number of foci/nucleus as

function of time post IR.

Figure 6. Assessment of the efficiency and accuracy of NHEJ in muscle stem cells. A) Satellite cells (FACS, *Tg:Pax7-nGFP* mice) were compared with MEFs after transfection with linearized or circular plasmid to calculate NHEJ efficiency, after plating for ampicillin (Amp) resistance (R) and chloramphenicol (Cm) sensitivity (S) (see supplementary material); **B)** Box plot (min to max) of NHEJ frequency in satellite cells (n=6 mice), and MEFs (n=3 independent cell cultures); **C)** Satellite cells (n=3 mice) and MEFs (n=3 experiments) were treated with DMSO or DNA-PK inhibitor NU7441 dissolved in DMSO; percentage inhibition of NHEJ (mean ± SD) calculated compared to control. NHEJ inhibition observed with MEFs is in agreement with previous data (Chayot, et al., 2012). **D)** Accurate repair events assayed by digestion of recovered plasmid with *EcoRV* (reconstitution of intact *EcoRV* site, see Fig. S6). Sequencing of several junctions confirmed accurate repair (not shown). Frequency of accurate events and events with micromodifications (±10 nucleotides) or detectable change in size of plasmid substrate (deletions) are shown. Repair events: n=144 for satellite cells and n=26 for MEFs. More than 96% of junctions in satellite cells and 100% in myoblasts were accurate; ~46% were accurate in MEFs. Mean ± SEM, unpaired t test, *** $p \leq 0.001$. Mean ± SD. **E)** Frequency of repair events in the presence of inhibitor NU7441. **F)** Sequences of clonal repair junctions (inaccurate events); an accurate repair event indicated on top. Columns 5'Δ and 3'Δ indicate number of deleted nucleotides; six nucleotides at junction site, shown for deletions > 23 nt. Microhomology is underlined in one DNA end, and size indicated in column MH. Nd= not determined. **G)** Scheme of prevalent types of junction reconstructed from sequencing clonal repair events. Top, blunt ends after EcoRV digestion and removal of intervening cassette. Single bases, vertical bars; with bases close to DNA termini in red (top strand) and blue (bottom strand). Pattern "a", accurate repair, ligation without processing of DNA ends. Pattern "b", inaccurate event (resection of two bases at each 3' end; synapsis with

2nt microhomology) generating a micro-modification. Pattern “c”, deletion of bases on both strands at each DNA termini; synapsis through microhomology (1-6 bp observed, 1bp shown).

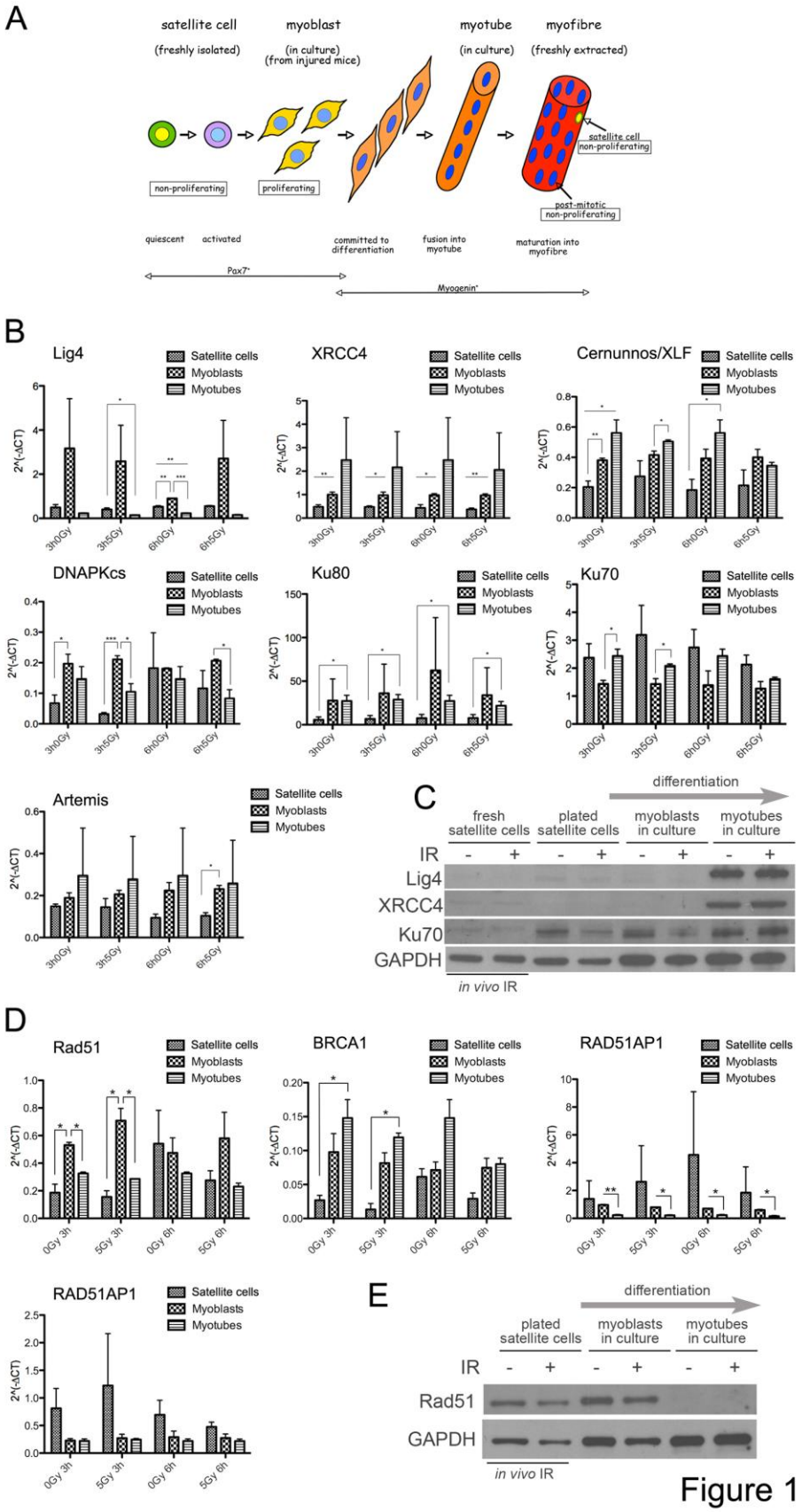
A
satellite cell
(freshly isolated)
myoblast
(in culture)
(from injured mice)
myotube
(in culture)
myofibre
(freshly extracted)
non-proliferating
proliferating
satellite cell
non-proliferating
post-mitotic
non-proliferating
quiescent
activated
committed to differentiation
fusion into myotube
maturation into myofibre
Pax7+
Myogenin+
B
Lig4
XRCC4
Cernunnos/XLF
DNAPKcs
Ku80
Ku70
Artemis
Satellite cells
Myoblasts
Myotubes
2^(-ΔCT)
3h0Gy
3h5Gy
6h0Gy
6h5Gy
C
differentiation
fresh satellite cells
plated satellite cells
myoblasts in culture
myotubes in culture
IR
Lig4
XRCC4
Ku70
GAPDH
in vivo IR
D
Rad51
BRCA1
RAD51AP1
0Gy 3h
5Gy 3h
0Gy 6h
5Gy 6h
E
differentiation
plated satellite cells
myoblasts in culture
myotubes in culture
IR
Rad51
GAPDH
in vivo IR

Figure 1

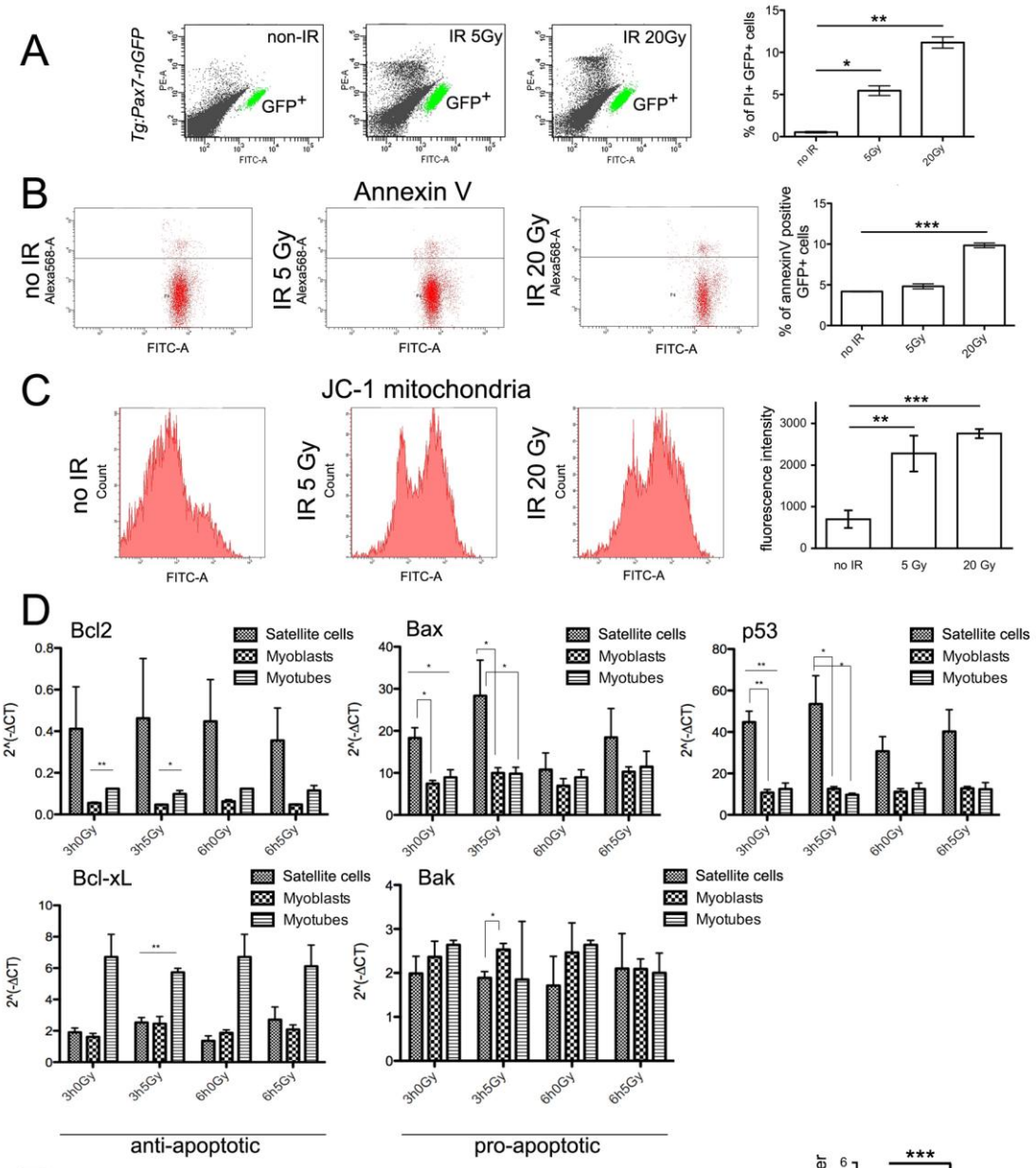
A
Tg:Pax7-nGFP
non-IR
IR 5Gy
IR 20Gy
GFP+
PE-A
FITC-A
% of PI+ GFP+ cells
no IR
5Gy
20Gy
B
Annexin V
no IR
IR 5 Gy
IR 20 Gy
Alexa568-A
FITC-A
% of annexinV positive GFP+ cells
C
JC-1 mitochondria
Count
fluorescence intensity
D
Bcl2
Bax
p53
Bcl-xL
Bak
Satellite cells
Myoblasts
Myotubes
2^(-ΔCT)
3h0Gy
3h5Gy
6h0Gy
6h5Gy
anti-apoptotic
pro-apoptotic
E
Hoechst / Pax7 / Myogenin
0h
72h
20 µm
nb Pax7+ cells per fiber
nb of+ cells per fiber
Pax7+
Myog+
Pax7+/Myog+
no IR +72h ex vivo
IR 5Gy x3 +72h ex vivo

Figure 2

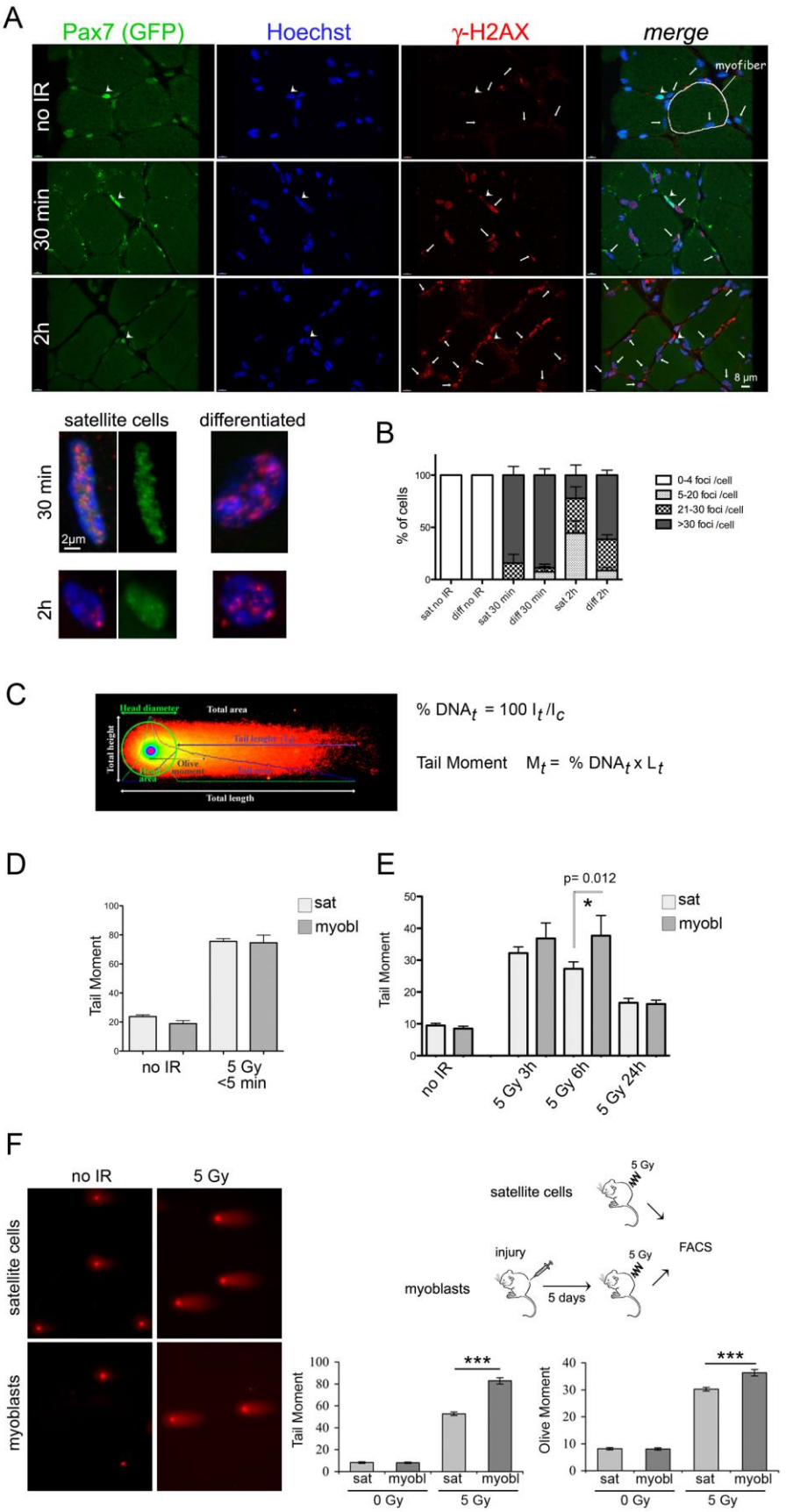
A
Pax7 (GFP)
Hoechst
γ-H2AX
merge
no IR
30 min
2h
myofiber
8 µm
satellite cells
differentiated
30 min
2µm
2h
B
% of cells
0-4 foci /cell
5-20 foci /cell
21-30 foci /cell
>30 foci /cell
sat no IR
diff no IR
sat 30 min
diff 30 min
sat 2h
diff 2h
C
Head diameter
Total area
Total height
Tail lenght
Olive moment
Total length
% DNA$_t$ = 100 I$_t$ /I$_c$
Tail Moment M$_t$ = % DNA$_t$ x L$_t$
D
Tail Moment
sat
myobl
no IR
5 Gy <5 min
E
p= 0.012
*
Tail Moment
sat
myobl
no IR
5 Gy 3h
5 Gy 6h
5 Gy 24h
F
no IR
5 Gy
satellite cells
myoblasts
satellite cells
5 Gy
injury
5 Gy
FACS
myoblasts
5 days
Tail Moment
***
sat
myobl
sat
myobl
0 Gy
5 Gy
Olive Moment
***
sat
myobl
sat
myobl
0 Gy
5 Gy

Figure 3

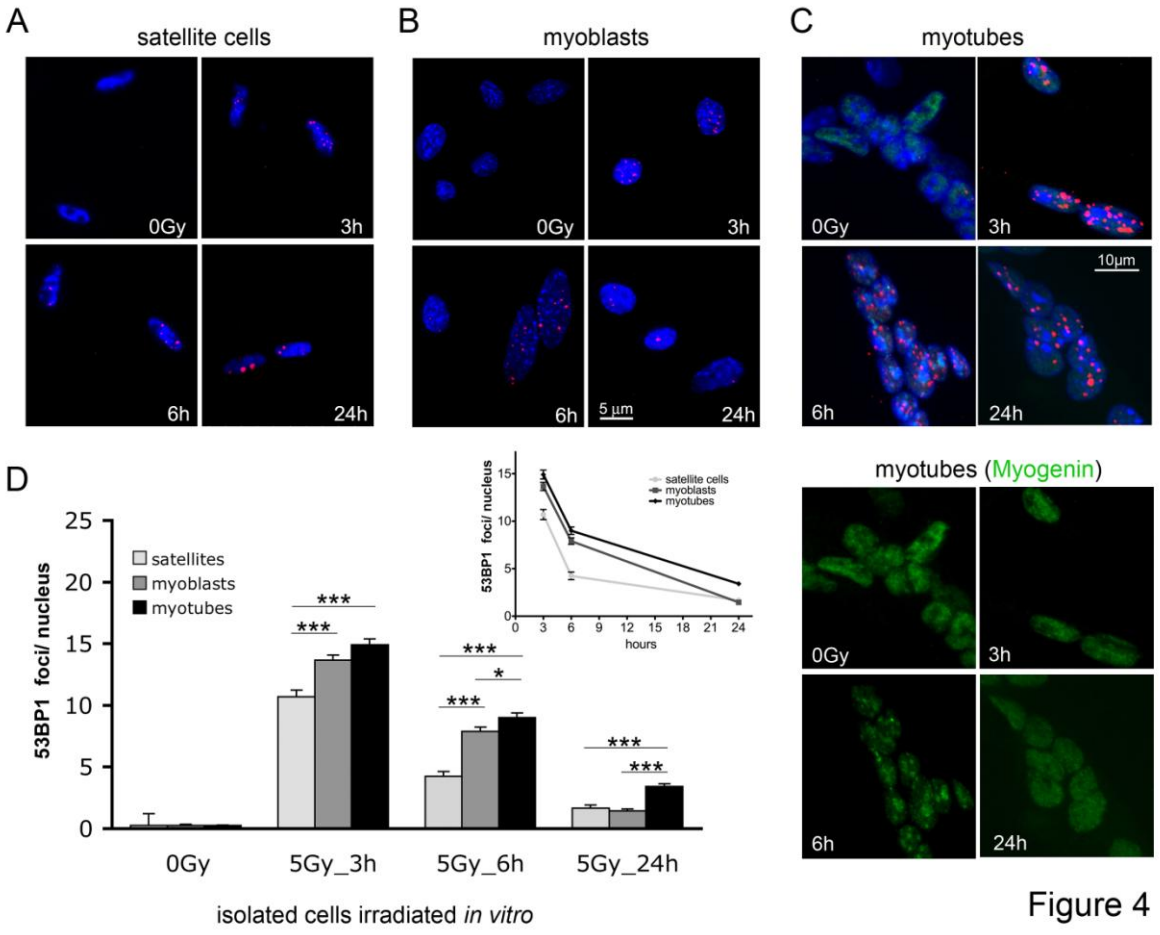

Figure 4

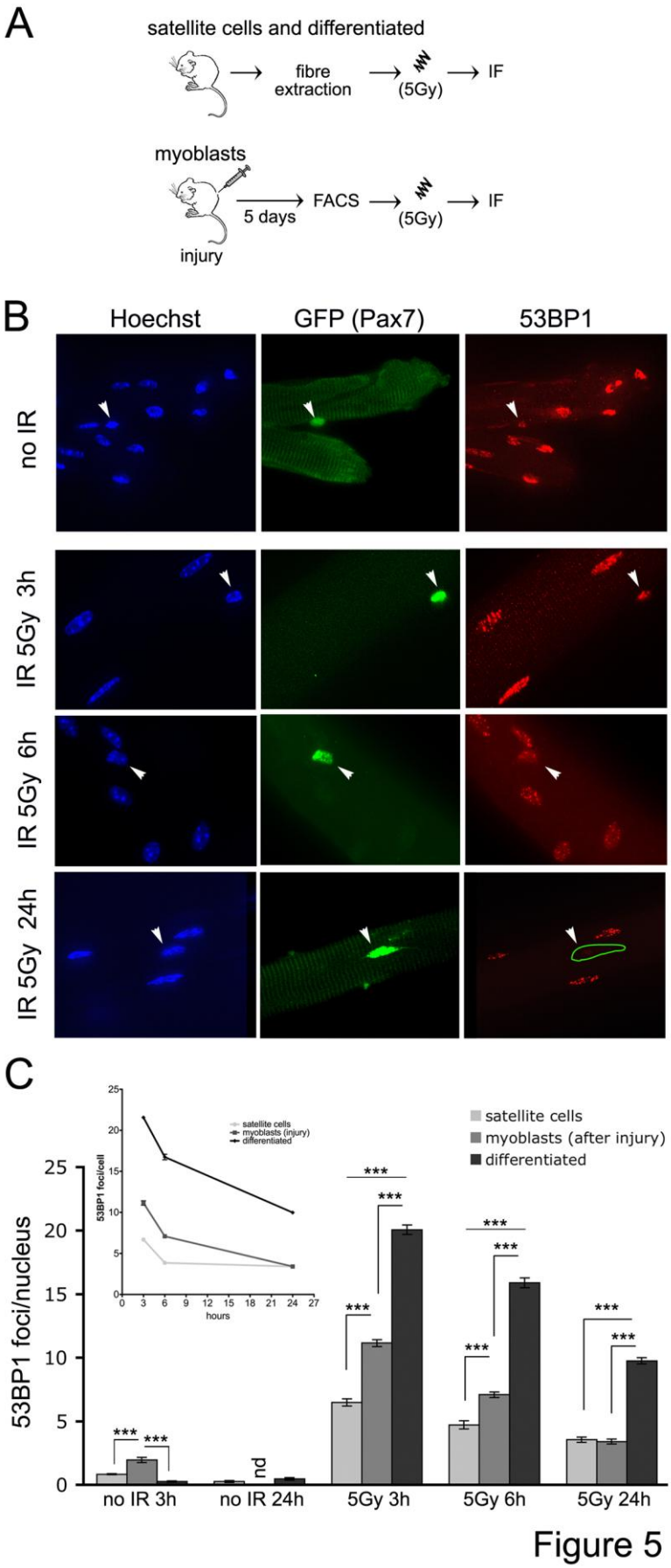
A
satellite cells and differentiated
fibre extraction
(5Gy)
IF
myoblasts
5 days
FACS
(5Gy)
IF
injury
B
Hoechst
GFP (Pax7)
53BP1
no IR
IR 5Gy 3h
IR 5Gy 6h
IR 5Gy 24h
C
satellite cells
myoblasts (after injury)
differentiated
53BP1 foci/nucleus
53BP1 foci/cell
hours
nd
no IR 3h
no IR 24h
5Gy 3h
5Gy 6h
5Gy 24h

Figure 5

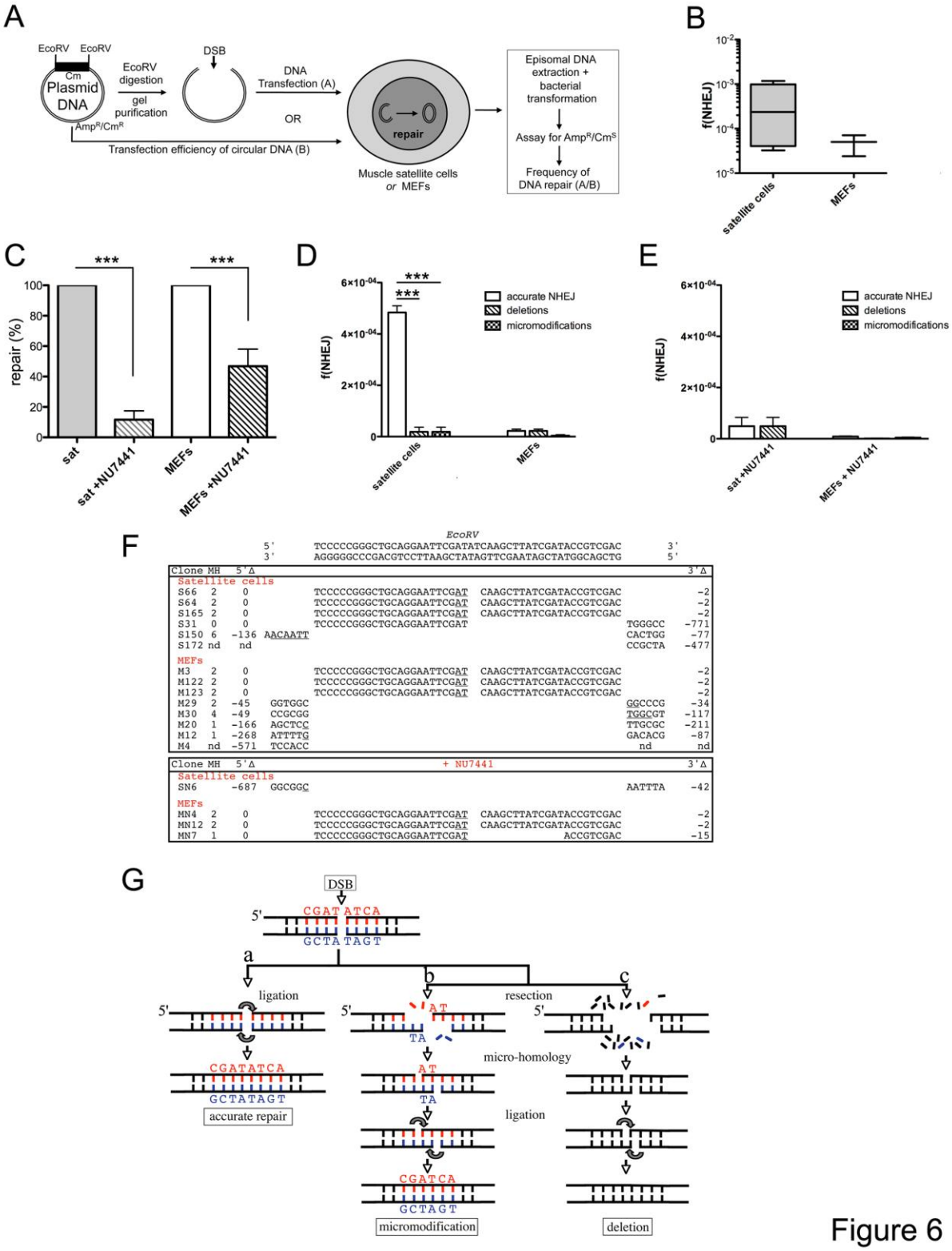

F

EcoRV

```
5'  TCCCCCGGGCTGCAGGAATTCGATATCAAGCTTATCGATACCGTCGAC  3'
3'  AGGGGGCCCGACGTCCTTAAGCTATAGTTCGAATAGCTATGGCAGCTG  5'
```

Clone	MH	5'Δ				3'Δ
Satellite cells						
S66	2	0	TCCCCCGGGCTGCAGGAATTCGAT	CAAGCTTATCGATACCGTCGAC		-2
S64	2	0	TCCCCCGGGCTGCAGGAATTCGAT	CAAGCTTATCGATACCGTCGAC		-2
S165	2	0	TCCCCCGGGCTGCAGGAATTCGAT	CAAGCTTATCGATACCGTCGAC		-2
S31	0	0	TCCCCCGGGCTGCAGGAATTCGAT		TGGGCC	-771
S150	6	-136 AACAATT			CACTGG	-77
S172	nd	nd			CCGCTA	-477
MEFs						
M3	2	0	TCCCCCGGGCTGCAGGAATTCGAT	CAAGCTTATCGATACCGTCGAC		-2
M122	2	0	TCCCCCGGGCTGCAGGAATTCGAT	CAAGCTTATCGATACCGTCGAC		-2
M123	2	0	TCCCCCGGGCTGCAGGAATTCGAT	CAAGCTTATCGATACCGTCGAC		-2
M29	2	-45 GGTGGC			GGCCCG	-34
M30	4	-49 CCGCGG			TGGCGT	-117
M20	1	-166 AGCTCC			TTGCGC	-211
M12	1	-268 ATTTTG			GACACG	-87
M4	nd	-571 TCCACC			nd	nd

Clone	MH	5'Δ	+ NU7441		3'Δ
Satellite cells					
SN6		-687 GGCGGC		AATTTA	-42
MEFs					
MN4	2	0	TCCCCCGGGCTGCAGGAATTCGAT	CAAGCTTATCGATACCGTCGAC	-2
MN12	2	0	TCCCCCGGGCTGCAGGAATTCGAT	CAAGCTTATCGATACCGTCGAC	-2
MN7	1	0	TCCCCCGGGCTGCAGGAATTCGAT	ACCGTCGAC	-15

Figure 6

Highlights

- DSB repair efficiency decreases as a function of differentiation in muscle cells
- Repair efficiency is not dependent on quiescence
- High repair efficiency is satellite cell is independent of the niche
- Satellite cells repair DSBs faithfully at the molecular level
- DSB repair depends on classical non-homologous end-joining factor DNA-PKcs